Journal of Solid State Chemistry **146,** 355–362 (1999)
Article ID jssc.1999.8362, available online at http://www.idealibrary.com on IDEAL®

Superspace-Group Approach to the Phase Transition of Cu_8GeSe_6

Mitsuko Onoda,[1] Motohiko Ishii, Philip Pattison,* Kenji Shibata, Akiji Yamamoto, and Gervais Chapuis*

*National Institute for Research in Inorganic Materials, Namiki, Tsukuba, 305-0044, Japan; and *Institute of Crystallography, University of Lausanne, BSP, CH-1015, Lausanne, Switzerland*

Received January 20, 1999; in revised form April 20, 1999; accepted May 7, 1999

The high- and low-temperature forms, i.e., phase I (stable above 328 K) and phase II (stable below 328 K), of Cu_8GeSe_6 have been investigated by the powder X-ray diffraction method. Cu_8GeSe_6 II is hexagonal with $A = 12.6438(2)$, $C = 11.7570(1)$ Å, $Z = 6$, and $P6_3cm$, and its structure is considered to be a superstructure of the high-temperature form, Cu_8GeSe_6 I (hexagonal, $a = 7.3164(4) \cong A/\sqrt{3}$, $c = 11.7679(7)$ Å, $Z = 2$, and $P6_3mc$). Rietveld analysis of Cu_8GeSe_6 I (350 K) and II (290 K) has been performed using diffraction data measured by a high-resolution powder diffractometer and synchrotron X-ray radiation. For Cu_8GeSe_6 II, a four-dimensional superspace group for commensurate modulation, $P6_3mc$(1/3 1/3 0), with basic cell constants $a = 7.2999$, $c = 11.7570$ Å has been successfully applied ($R_{wp} = 0.054$). The superspace-group description allows uniform treatment of both forms, and the phase transition of Cu_8GeSe_6 is explained in terms of the presence and absence of commensurate modulation waves. © 1999 Academic Press

INTRODUCTION

The ternary selenide containing Cu ions, Cu_8GeSe_6, crystallizes in a hexagonal system (1), differing from other compounds with the composition Cu_8MX_6 (M = Si, Ge; X = S, Se). Cu_8SiS_6, Cu_8SiSe_6, and Cu_8GeS_6 belong to an argyrodite family whose basic structures are described by a cubic system with $a \sim 9.9$ Å, and they exhibit respective phase transitions at approximate 330 K (2–8). In hexagonal Cu_8GeSe_6, a reversible phase transition at 328 K was reported, and the low- and high-temperature phases were examined, respectively, using the precession photograph and the Guinier-camera methods (1). Recently, the same group described the crystal structures of high- and low-temperature phases using a single crystal X-ray diffraction method: the high-temperature form, Cu_8GeSe_6 I, hexagonal with $a = 7.307(3)$, $c = 11.75(1)$ Å and $P6_3mc$; the low-temperature form, Cu_8GeSe_6 II, hexagonal with $a = 12.648(5) = 7.303(3) \times \sqrt{3}$, $c = 11.76(4)$ Å and $P6_3cm$ (9). Cu positions in Cu_8GeSe_6 I were expressed by four kinds of 6(c) of $P6_3mc$ with respective occupation factors 2/3, 1/3, 2/3, and 1.0. Those of Cu_8GeSe_6 II are in two 6(c) and three 12(d) of $P6_3cm$ and their occupancies are all 1.0.

Due to recent progress in the theoretical and experimental methods, it has become feasible to investigate the low-temperature phase from powder diffraction data. The low-temperature form is regarded as a superstructure, namely, a commensurately modulated structure of the high-temperature form of Cu_8GeSe_6. An application of the superspace-group theory may be advantageous in phase transition study even in the commensurate case. Selecting the initial parameters of the low-temperature structure may become simpler in high-dimensional formalism than those in three-dimensional formalism. In addition, the basic or average structure can be closely connected with the high-temperature form.

In the course of the phase relationship study in the Cu–Ge–Se system, a powder specimen of Cu_8GeSe_6 was synthesized. In the preliminary Rietveld analysis of the room-temperature form of Cu_8GeSe_6, it was very difficult to obtain a convergence. An application of the superspace-group theory might overcome this difficulty, as it has been revealed that four-dimensional approaches often lead to smooth convergence in structural refinements of modulated structures from unsatisfactory starting parameters. When dealing with high- and low-temperature phases, it is sometimes easier to measure a powder diffraction pattern than to obtain single-crystal diffraction data. This is one way to avoid twinning problems. If the Rietveld analysis based on the superspace-group approach is shown to be valid in the analysis of the superstructure, it will become a powerful method for studying phase transitions. We therefore propose to use X-ray powder diffraction data of Cu_8GeSe_6 I and II as a demonstration of the versatility of the superspace-group approach.

In this study, Rietveld analyses of Cu_8GeSe_6 I (350 K) and II (290 K) were performed based on data measured by

[1] To whom correspondence should be addressed. Fax: 81-298-58-5641. E-mail: onodam@nirim.go.jp.

0022-4596/99 $30.00

a high-resolution powder diffractometer and synchrotron X-ray radiation. The computer program PREMOS (10) based on the superspace-group approach was used. The structural models of Cu_8GeSe_6 I and II are described, respectively, in space group $P6_3mc$ with cell constants $a = 7.3164$ and $c = 11.7679$ Å and the four-dimensional superspace group for the commensurate modulation $P6_3mc(1/3\ 1/3\ 0)$ with basic cell constants $a = 7.2999$ and $c = 11.7570$ Å.

EXPERIMENTAL

Cu_8GeSe_6 powder was prepared by reacting stoichiometric amounts of Cu_2Se (99.9%), Ge (99.9%), and Se (99.9%) in an evacuated and sealed silica tube for 4 days at 773 K. The sample was identified by using conventional powder X-ray diffraction pattern. The reversible phase transition at about 328 K with an enthalpy change of approximately 6 J/g was confirmed by a differential scanning calorimetory (DSC) measurement. The specimen sealed into a glass capillary with a diameter of 0.3 mm was set in the high-resolution powder diffraction instrument installed at the Swiss–Norwegian beam line (BM1B) at the European Synchrotron Radiation Facilities (ESRF). Step-scan data of the high-temperature phase Cu_8GeSe_6 I and the low-temperature phase Cu_8GeSe_6 II were obtained, respectively, using the wave lengths 0.6479(1) Å at 350 K and 0.6505(1) Å at 290 K. The wavelength was checked before each measurement using a Si powder standard. In each case, the sample was enclosed in an oven with a temperature stability better than ± 0.5 K. Some measurement conditions are summarized in Table 1.

SYMMETRY CONSIDERATIONS

All reflections in the pattern of Cu_8GeSe_6 I measured at 350 K could be indexed by selecting a hexagonal cell with $a = 7.3164$ and $c = 11.7679$ Å. The reflection condition $l = 2n$ for hhl seems to be valid. The possible space groups are $P6_3/mmc$ and its subgroups. Considering the likelihood of Se arrangement related to an $2H$-type Friauf–Laves phase in analogy with the argyrodite-type structure (4), the most probable space group of the phase I is $P6_3mc$ as used by Jaulmes *et al.* (9).

TABLE 1
Conditions of Powder X-Ray Diffraction Data Collection

Specimen	Synthesized Cu_8GeSe_6 powder
Shape of specimen	Sealed in a glass capillary (0.3 mm diameter) in an oven
Instrument	High-resolution powder diffraction instrument on beam line BM1B at the ESRF (Grenoble)
Radiation source	Synchrotron
Wavelength (Å)	0.6479(1) (350 K), 0.6505(1) (290 K)
Step size (°)	0.005
Monochromator	Si(111)
Analyzer	Si (111)
Range of 2θ(°)	3.0–33.845
Range of d-spacings (Å)	12.4–1.116
Maximum intensity	2579 c/s.(350 K), 6051 c/s.(290 K)

Most of the strong reflections of the room-temperature phase Cu_8GeSe_6 II measured at 290 K can be indexed from a hexagonal cell ($a = 7.2999$, $c = 11.7570$ Å), and all peaks can be assigned to the hexagonal cell with $A = 12.6438 = 7.2999 \times \sqrt{3}$ and $C = 11.7570$ Å. The reflection condition $L = 2n$ for $H\bar{H}L$ seems to exist. To apply four-dimensional formalism, the basic cell with the axes $\mathbf{a} = (2\mathbf{A} + \mathbf{B})/3$, $\mathbf{b} = (-\mathbf{A} + \mathbf{B})/3$, and $\mathbf{c} = \mathbf{C}$ is adopted. Using the modulation wave vector given by $\mathbf{q} = \mathbf{A}^* = (\mathbf{a}^* + \mathbf{b}^*)/3$, each reflection is expressed by $\mathbf{h} = h\mathbf{a}^* + k\mathbf{b}^* + l\mathbf{c}^* + m\mathbf{q}$ using the four integers, h, k, l, and m, where $\mathbf{a}^*$, $\mathbf{b}^*$, and $\mathbf{c}^*$ are the reciprocal vectors corresponding to $\mathbf{a}$, $\mathbf{b}$, and $\mathbf{c}$. As the systematic reflection condition changes from $L = 2n$ for $H\bar{H}L$ to $l = 2n$ for hhl, the space group of the basic structure is $P6_3/mmc$ or its subgroups. As the basic structure of Cu_8GeSe_6 II is closely related to the structure of Cu_8GeSe_6 I, the most probable space group is $P6_3mc$. From the relationships $\mathbf{A}^* = \mathbf{q}$ and $\mathbf{B}^* = (2\mathbf{b}^* - \mathbf{a}^*)/3 = \mathbf{b}^* - \mathbf{q}^*$, the relationships between the coordinates $X = u$, and $Y = y - u$ are derived where u is the fourth coordinate. Using these relationships, a group of symmetry operations whose generator set is $-y, x-y, z, u-y$; $-x, -y, z+1/2, -u$; $-y, -x, z, -u$ has been obtained for the four-dimensional superspace group for commensurate modulation with $\mathbf{q} = (\mathbf{a}^* + \mathbf{b}^*)/3$, and it is expressed by the symbol $P6_3mc(1/3\ 1/3\ 0)$.

Besides the restriction conditions for the Fourier amplitudes of the modulation functions for an incommensurate structure, some additional restrictions are needed for commensurate modulation because of the presence of equivalent modulation waves. After calculating the equivalent modulation waves and their constraints on parameters using the program SPL (11), the restriction conditions for atoms in special positions were obtained by unifying the constraints. The results of the symmetry considerations for Cu_8GeSe_6 I and II are summarized in Table 2 together with the three-dimensional symmetry of Cu_8GeSe_6 II.

RIETVELD ANALYSIS

Powder diffraction data were obtained from a high-resolution diffractometer and synchrotron X-ray source. Although the narrow widths of reflections allow a reliable analysis of complex crystal structures, large fluctuations in the background caused by statistical variation in the background counts are often observed. Because fluctuation in

TABLE 2
Results of Symmetry Considerations for Cu_8GeSe_6 I and Cu_8GeSe_6 II

	Cu_8GeSe_6 I	Cu_8GeSe_6 II	
	Three-dimensional	Four-dimensional	Three-dimensional
(a) Lattice constants			
	$a = 7.3164(4)$,	$a = 7.2999(1)$,	$A = 7.2999\sqrt{3} = 12.6438(2)$,
	$b = 7.3164$,	$b = 7.2999$,	$B = 7.2999\sqrt{3} = 12.6438$,
	$c = 11.7679(7)$ Å	$c = 11.7570(1)$ Å $\mathbf{q} = (\mathbf{a}^* + \mathbf{b}^*)/3$	$C = 11.7570(1)$ Å
(b) Symmetry			
Generator set of symmetry operations	$-y, x-y, z$ $-x, -y, 1/2+z$ $-y, -x, z$	$-y, x-y, z, -y+u$ $-x, -y, 1/2+z, -u$ $-y, -x, z, -u$	$-Y, X-Y, Z$ $-X, -Y, 1/2+Z$ Y, X, Z
Symbol	$P6_3mc$	$P6_3mc(1/3\ 1/3\ 0)$	$P6_3cm$
(c) Systematic reflection conditions			
	hhl	$hhlm$	$H\bar{H}L$
	$l = 2n$	$l = 2n$	$L = 2n$
(d) Atomic positions			
Ge	$0, 0, z$	$0, 0, z$	0, 0, Z; 1/3, 2/3, Z
Se1	$0, 0, z$	$0, 0, z$	0, 0, Z; 1/3, 2/3, Z
Se2	$1/3, -1/3, z$	$1/3, -1/3, z$	$X, 0, Z$
Se3	$x, -x, z$	$x, -x, z$	$X, 0, Z$; X, Y, Z
Se4	$1/3, -1/3, z$	$1/3, -1/3, z$	$X, 0, Z$
Cu1	$x, -x, z$	$x, -x, z$	X, Y, Z
Cu2	$x, -x, z$	$x, -x, z$	$X, 0, Z$; X, Y, Z
Cu3	$x, -x, z$	$x, -x, z$	$X, 0, Z$; X, Y, Z

(e) Requirements for the atomic parameters of Cu_8GeSe_6 II in four-dimensional formalism. ($A_{1,i}$ and $B_{1,i}$ ($i = x, y, z, B$) are the cosine and sine amplitudes of the Fourier series with wave vector $\mathbf{q} = (\mathbf{a}^* + \mathbf{b}^*)/3$.)

Ge	$A_{1,x} = B_{1,x} = A_{1,y} = B_{1,y} = 0,\ B_{1,z} = 0$
Se1	$A_{1,x} = B_{1,x} = A_{1,y} = B_{1,y} = 0,\ B_{1,z} = 0$
Se2	$B_{1,x} = B_{1,y} = A_{1,x}\sqrt{3} = -A_{1,y}\sqrt{3},\ A_{1,z} = B_{1,z} = 0$
Se3	$A_{1,x} = -A_{1,y},\ B_{1,x} = B_{1,y},\ B_{1,z} = 0$
Se4	$B_{1,x} = B_{1,y} = A_{1,x}\sqrt{3} = -A_{1,y}\sqrt{3},\ A_{1,z} = B_{1,z} = 0$
Cu1	$A_{1,x} = -A_{1,y},\ B_{1,x} = B_{1,y},\ B_{1,z} = 0,\ B_{1,B} = 0$
Cu2	$A_{1,x} = -A_{1,y},\ B_{1,x} = B_{1,y},\ B_{1,z} = 0,\ B_{1,B} = 0$
Cu3	$A_{1,x} = -A_{1,y},\ B_{1,x} = B_{1,y},\ B_{1,z} = 0,\ B_{1,B} = 0$

the background may be responsible for the unfavorable reliability factor and large standard deviations of the parameters, three-point smoothing data were used for the present Rietveld analysis using the program PREMOS (10).

The structural model of the high-temperature form (Cu_8GeSe_6 I) was described by using the following positions of $P6_3mc$: 2Ge in 2(*a*), 2Se in 2(*a*), 4Se in two 2(*b*), 6Se in 6(*c*), 4Cu in 6(*c*) with occupation factor 2/3 and 12Cu in two 6(*c*). Individual isotropic thermal parameters for the three Cu ions are used besides an isotropic parameter for the Ge atom and one common isotropic parameter for the three Se atoms. Fairly good agreement was obtained, yielding an $R_{wp} = 0.074$.

The starting parameters of the room-temperature phase (Cu_8GeSe_6 II) were derived from the model of Cu_8GeSe_6 I, using the same positional and thermal parameters. The cosine and sine terms of the Fourier amplitudes A_0, A_1, and B_1 of the modulation functions are selected as variable parameters by considering the structural degree of freedom, where the suffixes m represent the wave vectors $m\mathbf{q} = m(\mathbf{a}^* + \mathbf{b}^*)/3$. The requirements listed in Table 2e are used. Convergence from the initial parameters was obtained rapidly and smoothly through several cycles. The reliability factor obtained is $R_{wp} = 0.056$.

The Rietveld analysis patterns and the final parameters of Cu_8GeSe_6 I and II are shown in Fig. 1 and Table 3. From the parameters of Table 3, selective interatomic distances have been calculated, as shown in Table 4, using the program PRJMS (10).

DISCUSSION

Crystal structural models of Cu_8GeSe_6 I and II are illustrated in Fig. 2 using the parameters of Table 3. They agree closely with the respective crystal structures analyzed by Jaulmes *et al.* (9) using the single-crystal X-ray diffraction data and three-dimensional formalism. The framework structures of Cu_8GeSe_6 I and II consisting of Ge and Se atoms are similar to each other, as shown in Fig. 2, and they are of the same type as the atomic arrangement of the 2*H*-type Friauf–Laves phase (12). The chalcogen arrangement of the argyrodite-family is of the same type as the atomic arrangement of the 3*C*-type Friauf–Laves phase, as described by Kuhs *et al.* (4). Friauf–Laves phases form the structures in which the "kagome" nets and the less dense triangular nets of atoms stack alternately and in which all interstices are tetrahedral (13, 14). Such a network structure of Se in which all interstices are tetrahedral is present in Cu_8GeSe_6, and two kinds of nearly regular tetrahedral sites, one for Ge and the other vacant, are formed by Se1 and Se3. Se2 and Se4 lie in centers of the interpenetrating Se–Se Friauf-type polyhedra.

The crystal structure of the low-temperature phase (Cu_8GeSe_6 II) could be analyzed successfully using the powder diffraction data, although a superstructural analysis using the Rietveld method is usually difficult because of the overlap of reflections and a large number of initial positional parameters. In a structural refinement, the four-dimensional approach often leads to a smooth convergence from approximate initial parameters, and this character is also demonstrated in the present case. The low-temperature form often crystallizes in twin or multiple-twin forms (8). As twinning has often serious effects on structural analysis based on single-crystal diffraction data, the procedure by which a low-temperature form can be successfully analyzed from powder diffraction data will be helpful in the study of phase transitions, although the present specimen is not

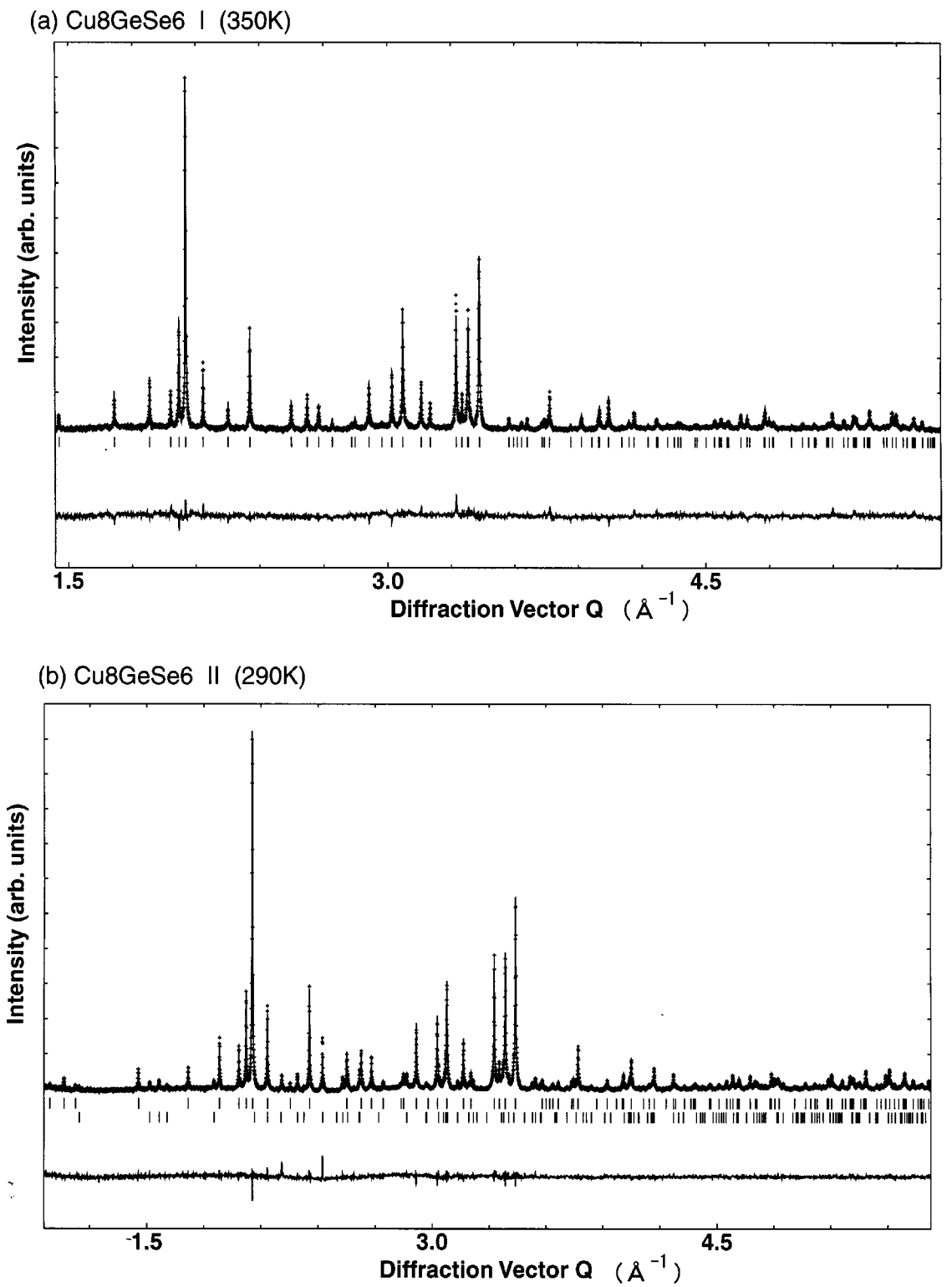

FIG. 1. The Rietveld patterns of (a) Cu_8GeSe_6 I (350 K, $\lambda = 0.6479(1)$ Å) and (b) Cu_8GeSe_6 II (290 K, $\lambda = 0.6505(1)$ Å) based on the data measured on the high-resolution powder diffraction instrument installed on beam line BM1B at the ESRF. The patterns are plotted using the diffraction vector length $Q\,(=2\pi/d)$ Å^{-1} as the x axis. The vertical lines below the profiles indicate the positions of (a) the reflections and (b) the main (upper) and superreflections (lower).

TABLE 3
Structural Model of Cu_8GeSe_6 I and II Described Using the Positions of $P6_3mc$: 2Ge in 2(*a*), 2Se in 2(*a*), 4Se in Two 2(*b*), 6Se in 6(*c*), 4Cu in 6(*c*) and 12Cu in Two 6(*c*).

		x	*y*	*z*	*B* (Å^2)	Occupancy
(a) The high-temperature phase (Cu_8GeSe_6 I, 350 K)						
Ge		0.0	0.0	0.202(6)	1(1)	1.0
Se1		0.0	0.0	0.0	1.1(6)	1.0
Se2		1/3	−1/3	0.450(8)	1.1[6]	1.0
Se3		−0.179(2)	0.179[2]	0.249(5)	1.1[6]	1.0
Se4		1/3	−1/3	0.084(6)	1.1[6]	1.0
Cu1		−0.472(6)	0.472[6]	0.096(9)	6(2)	2/3
Cu2		0.462(4)	−0.462[4]	0.306(5)	4(2)	1.0
Cu3		−0.187(4)	0.187[4]	0.454(7)	5(1)	1.0
(b) The room-temperature phase (Cu_8GeSe_6 II, 290 K)[a]						
Ge	fundamental	0.0	0.0	0.20	0.8(7)	1.0
	A_0	0.0	0.0	−0.001(3)		
	A_1	0.0	0.0	0.009(7)		
	B_1	0.0	0.0	0.0		
Se1	fundamental	0.0	0.0	0.0	0.2(3)	1.0
	A_0	0.0	0.0	0.0		
	A_1	0.0	0.0	0.011(4)		
	B_1	0.0	0.0	0.0		
Se2	fundamental	1/3	−1/3	0.45	0.2[3]	1.0
	A_0	0.0	0.0	0.007(4)		
	A_1	0.027(2)	−0.027[2]	0.0		
	B_1	0.046[4]	0.046[4]	0.0		
Se3	fundamental	−0.2	0.2	0.25	0.2[3]	1.0
	A_0	0.020(1)	−0.020[1]	−0.002(3)		
	A_1	−0.001(3)	0.001[3]	0.012(3)		
	B_1	−0.009[5]	−0.009[5]	0.0		
Se4	fundamental	1/3	−1/3	0.08	0.2[3]	1.0
	A_0	0.0	0.0	0.005(4)		
	A_1	0.009(3)	−0.009[3]	0.0		
	B_1	0.016(6)	0.016[6]	0.0		
Cu1	fundamental	−0.5	0.5	0.08	1.0	2/3
	A_0	0.020(2)	−0.020[2]	−0.006(3)	0.8(9)	0.0
	A_1	0.0	0.0	0.0	0.0	−2/3
	B_1	0.041(6)	0.041[6]	0.0	0.0	0.0
Cu2	fundamental	0.5	−0.5	0.31	1.0	1.0
	A_0	−0.038(1)	0.038[1]	0.006(4)	0.2(6)	
	A_1	−0.018(2)	0.018[2]	−0.046(3)	−1.1(9)	
	B_1	0.008(7)	0.008[7]	0.0	0.0	
Cu3	fundamental	−0.2	0.2	0.45	1.0	1.0
	A_0	0.015(1)	−0.015[1]	0.003(4)	0.3(7)	
	A_1	0.001(3)	−0.001[3]	0.019(4)	−1.2(9)	
	B_1	0.070(5)	0.070[5]	0.0	0.0	

Note. The independent and propagated standard deviations are given in parentheses and square brackets, respectively. The isotropic thermal parameters, B(Ge) and B(Se), are used common to all Ge and all Se ions, respectively, and individual isotropic thermal parameters are adopted for Cu ions.

[a] A_m and B_m are the amplitudes of the cosine and sine terms with wave vector $m\mathbf{q} = m(\mathbf{a}^* + \mathbf{b}^*)/3$ in the modulation function expressed as a Fourier series. To obtain the parameter values of the average structure, the values of A_0 should be added to the corresponding fundamental values.

TABLE 4
Interatomic Distances (Å) Calculated from the Parameters Listed in Table 3

(a) The high-temperature phase (Cu_8GeSe_6 I, 350 K)

(1) $GeSe_4$ tetrahedral unit

Ge–Se1	2.38	Se1–Se3,Se3^1,Se3^2	3.71 × 3
–Se3,Se3^1,Se3^2	2.34 × 3	Se3–Se3^1,Se3^2	3.94 × 2
		Se3^1–Se3^2	3.94

(2) Cu–Se (< 2.9Å)

Cu1–Se2^3	2.46	Cu2–Se2	2.36	Cu3–Se1^9	2.44
–Se3^4,Se3^5	2.59 × 2	–Se3^7,Se3^8	2.43 × 2	–Se3	2.41
–Se4^6	2.47			–Se4^9	2.40

(3) Cu–Cu(< 3.0Å)

Cu1–Cu2^6	2.60	Cu2–Cu1^6	2.60	Cu3–Cu1^{14},Cu1^{15}	2.78×2
–Cu3^{10},Cu3^{11}	2.78 × 2	–Cu2^{12},Cu2^{13}	2.83 × 2	–Cu2^{16},Cu2^{17}	2.90 × 2
		–Cu3^7,Cu3^8	2.90 × 2		

(b) The room–temperature phase (Cu_8GeSe_6 II, 290 K)

(1) $GeSe_4$ tetrahedral unit

Ge–Se1	2.31	Se1–Se3,Se3^1,Se3^2	3.71 × 3
–Se3,Se3^1,Se3^2	2.30 × 3	Se3–Se3^1,Se3^2	3.97 × 2
		Se3^1–Se3^2	3.97
Ge*–Se1*	2.36	Se1*–Se3*,Se3^1*,Se3^2*	3.70 × 3
–Se3*,Se3^1*,Se3^2*	2.34 × 3	Se3*–Se3^1*,Se3^2*	3.94 × 2
		Se3^1*–Se3^2*	3.94

(2) Cu–Se (< 2.9Å)

		Cu2–Se2	2.45	Cu3–Se1^9	2.38
		–Se3^7,Se3^8	2.57 × 2	–Se3	2.50
		–Se4	2.52	–Se4^9	2.40
Cu1*–Se2^3*	2.44	Cu2*–Se2*	2.38	Cu3*–Se1^9*	2.47
–Se3^4*	2.56	–Se3^7*	2.47	–Se3*	2.42
–Se4^6*	2.43	–Se3^8*	2.44	–Se4^9*	2.48

(3) Cu–Cu(< 3.0Å)

		Cu2–Cu2^{12},Cu2^{13}	2.83 × 2	Cu3–Cu1^{14},Cu1^{15}	2.65 × 2
		–Cu3^7,Cu3^8	2.88 × 2	–Cu2^{16},Cu2^{17}	2.76 × 2
Cu1*–Cu2^6*	2.77	Cu2*–Cu^{16}*	2.77	Cu3*–Cu1^{15}*	2.86
–Cu3^{10}*	2.86	–Cu2^{13}*	2.83	–Cu2^{16}*	2.88
–Cu3^{11}*	2.65	–Cu3^7*	2.76	–Cu2^{17}*	2.91
		–Cu3^8*	2.91	–Cu3^5*	2.78

Note. Symmetry codes: (1) $-y, x-y, z$ (2) $-x+y, -x, z$ (3) $-x, -y, z-1/2$ (4) $-y, 1+x-y, z$ (5) $-x+y-1, -x, z$ (6) $x-1, y+1, z$ (7) $1-y, x-y, z$ (8) $-x+y, -1-x, z$ (9) $-x, -y, z+1/2$ (10) $y-1, -x+y, z-1/2$ (11) $x-y, x+1, z-1/2$ (12) $-y, x-y-1, z$ (13) $-x+y+1, -x, z$ (14) $y-1, -x+y-1, 1/2+z$ (15) $x-y+1, x+1, z+1/2$ (16) $-y-1, x-y-1, z$ (17) $-x+y+1, 1-x, z$ (*) $x+1, y+1, z$. Symmetry operators (1*), (2*) … (17*) represent, respectively, the products of operators (1), (2) … (17) with (*).

affected by twinning at the transition because high- and low-temperature structures have the same point groups 6*mm*.

Incommensurately modulated structures do not have three-dimensional periodicity; their symmetry can, however, be described by superspace groups based on $(3 + d)$ translations, where d is the number of independent modulation waves. A tabulation of all superspace groups for $d = 1$ is available (15–17). In the present case, Cu_8GeSe_6 I crystallizes in $P6_3mc$, and new reflections appear at positions $m\mathbf{q}$ with integer m and $\mathbf{q} = (\mathbf{a}^* + \mathbf{b}^*)/3$ in the diffraction pattern

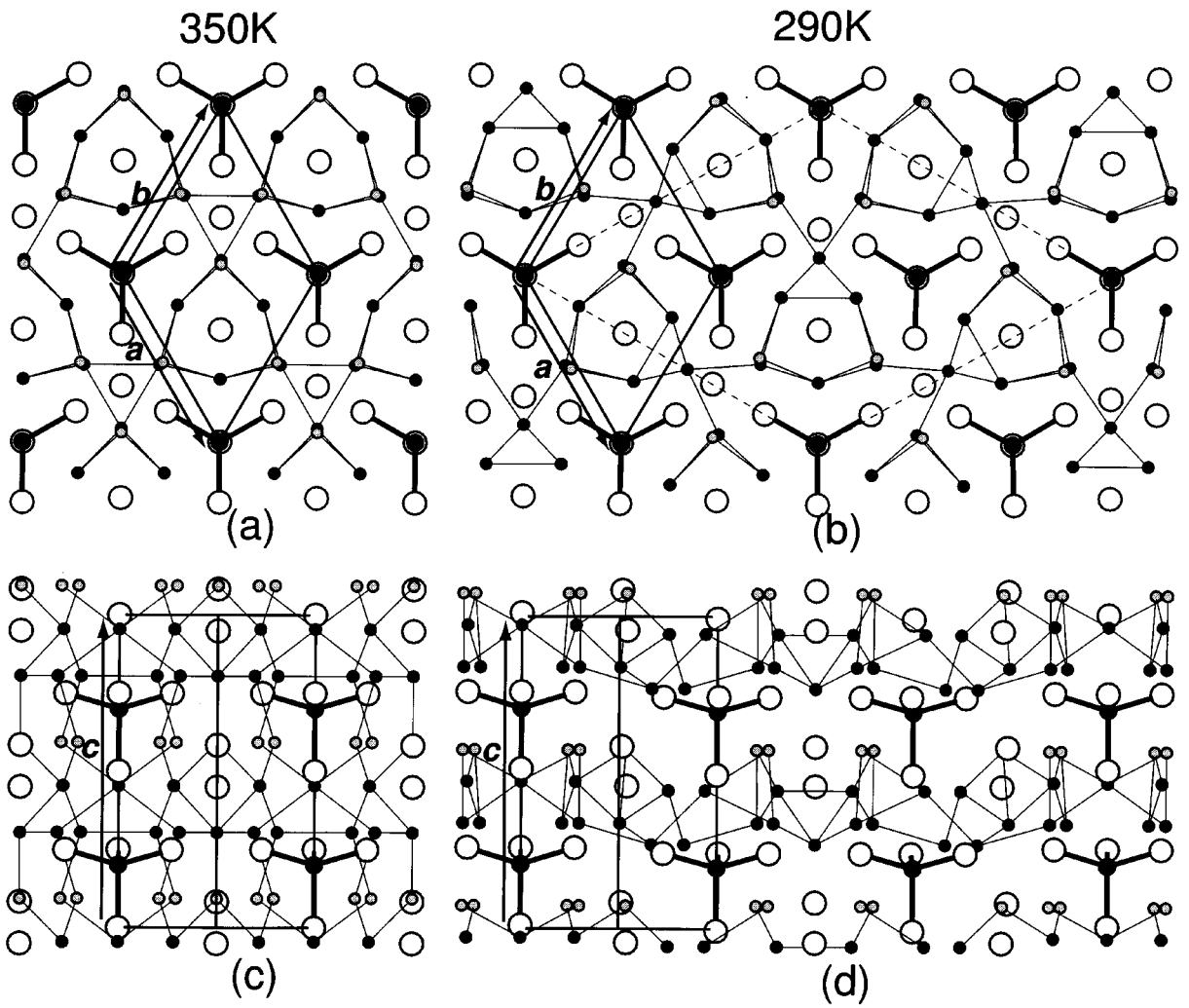

FIG. 2. Structures of (a) (c) Cu_8GeSe_6 I (350 K) and (b) (d) Cu_8GeSe_6 II (290 K) described in $P6_3mc$: 2Ge in 2(*a*), 2Se in 2(*a*), 4Se in two 2(*b*), 6Se in 6(*c*), 4Cu in 6(*c*) and 12Cu in two 6(*c*). (a), (b) and (c), (d) are, respectively, the bounded projections of $0.26 < z < 0.76$ and $-0.6 < x - y < 0.6$. The large open and medium solid circles represent Se and Ge, respectively. The small circles represent Cu positions: light shaded Cu1, dark shaded Cu2, and solid Cu3. Cu1 in (a) and (c) are partially occupied. Ge is joined with thick rods to the nearest Se, and Cu–Cu distances less than 3.0 Å are shown by thin rods. The thin broken lines in (b) represent the unit cell adopted by Jaulmes *et al.* (9).

of Cu_8GeSe_6 II, meaning that a commensurately modulated structure has been formed. The Bravais classes of superspace groups for particular commensurately modulated structures were reported previously (18), and the (3 + 1)D Bravais class of Cu_8GeSe_6 II is listed as No. 6 in the literature (18). The present study is the first example of Rietveld analysis using such a superspace-group description which is not included in the list of de Wolff *et al.* (15–17).

In four-dimensional formalism, the *x*, *y*, *z* components of the displacement vector from the fundamental structure of Cu_8GeSe_6 II are expressed by $c(\tau) = A_0 + A_1 \cos 2\pi\tau + B_1 \sin 2\pi\tau$, where $c = x, y, z$, and τ represents the phase of the modulation wave (19). In the commensurate structural case, the crystal appears as sections for constant discrete phases of the modulation wave. For Cu_8GeSe_6 II, the constant discrete phases are 0, 1/3, and 2/3. The corresponding translations in real space are (0, 0, 0)+, (1, 1, 0)+, and (2, 2, 0)+, and the displacement components from the fundamental structure are, respectively, expressed by $A_0 + A_1$, $A_0 - A_1/2 + B_1\sqrt{3}/2$, and $A_0 - A_1/2 - B_1\sqrt{3}/2$. In this way, each atomic position in $P6_3mc$(1/3 1/3 0) separates into two kinds of positions in $P6_3cm$ with a ratio of 1 to 2, as shown in Table 2(d). For the occupancy of Cu1 and isotropic thermal parameters of Cu1, Cu2, and Cu3, scalar modulation functions are used. Considering the commensurate modulation waves in $P6_3mc$(1/3 1/3 0), the first-order sine Fourier term *B* must be equal to zero for each Cu atom in

a special position. For the discrete phases 0, 1/3, and 2/3, occupancies of Cu1 are 0.0, 1.0, and 1.0, and isotropic thermal parameters of Cu1, Cu2, and Cu3 are expressed by $A_0 + A_1$, $A_0 - A_1/2$, and $A_0 - A_1/2$ using the parameter values listed in Table 3b.

Because of the Cu–ionic conductor character, the Cu distribution in the high-temperature phase can be approximately described by many partially occupied sites. In the previous work (9), the Cu positions in Cu_8GeSe_6 I were expressed successfully by four independent positions, with respective occupation factors 2/3, 1/3, 2/3, and 1.0. Although the choice of the same set of positional parameters in the Rietveld analysis of Cu_8GeSe_6 I will give satisfactory results, we prefer a smaller number of positions, namely, three independent positions with respective occupancies 2/3, 1.0, and 1.0, despite a small loss of convergence. They are the same types of positions as those of Cu_8GeSe_6 II listed in Table 3. The relationships between the structures of Cu_8GeSe_6 I and II are also better illustrated. Cu1 with occupancy 2/3 lies in a distorted Se–Se tetrahedron, and Cu2 and Cu3 lie near the centers of Se–Se triangles, respectively (Table 4a). In Cu_8GeSe_6 II, each of Cu2 and Cu3 separates into three positions with symmetry codes x, y, z, $x + 1, y + 1, z$ and $x + 2, y + 2, z$. The last two positions are equivalent in three-dimensional formalism, and one of them is listed in Table 4b with symmetry operation *. As a result of occupancy modulation, Cu1 with a symmetry code x, y, z vanishes, and Cu1* with codes $x + 1$, $y + 1$, z and $x + 2, y + 2, z$ remains with occupancies 1.0. As shown in Table 4b, Cu2 lies in a distorted Se–Se tetrahedron, and Cu3, Cu1*, Cu2*, and Cu3* lie in the vicinity of Se–Se triangle planes.

The narrow widths of reflections, even at high angle, have made possible adoption of individual thermal parameters for Cu ions. The individual thermal parameters of Cu ions are of interest because Cu_8GeSe_6 is expected to become a Cu–ionic conductor at elevated temperature, though the isotropic thermal parameters give modest information compared with anisotropic thermal parameters or nonharmonic atomic displacement factors which would have been refined using single-crystal diffraction data. In Cu_8GeSe_6 I, the isotropic thermal parameters of Cu ions are quite large; $B(Cu1) = 6$, $B(Cu2) = 4$, and $B(Cu3) = 5$ Å^2. Such large thermal parameters can be understood in terms of possible thermal anharmonicity and/or short-range disorder. In Cu_8GeSe_6 II, the isotropic thermal parameters of Cu ions are modulated relative to their average values; $B(Cu2) = 0.1$, $B(Cu3) = 0.1$, $B(Cu1*) = 1.8$, $B(Cu2*) = 1.8$, and $B(Cu3*) = 1.9$ Å^2. Coordination states around Cu ions, particularly Cu–Cu linkage, seem to affect thermal parameters, as shown in Table 4(b), as Cu1*, Cu2*, and Cu3* have respective nonsymmetrical coordination patterns showing larger thermal parameters than those of Cu2 and Cu3 in highly symmetrical positions.

The average structure of Cu_8GeSe_6 II, where the positional parameters of all atoms and the thermal and occupational parameters of Cu are obtained as the sums of A_0 and the fundamental parameters listed in the corresponding columns of Table 3(b), is very close to the model of Cu_8GeSe_6 I. By adopting the superspace-group approach, the relationships between the atomic arrangements of Cu_8GeSe_6 II and I can be understood in terms of the existence and absence of commensurate modulation waves, whereas the model of Cu_8GeSe_6 I is described on the basis of the smaller number of atoms with large thermal parameters which can be related to thermal anharmonicity and/or short-range disorder. Table 4 shows that the number of Cu–Cu bonds with distances around 2.8 Å increases and that the short Cu–Cu bonds less than 2.7 Å decrease in Cu_8GeSe_6 II, as compared to the model of Cu_8GeSe_6 I. The main driving force for the modulation waves can thus be attributed to the Cu–Cu repulsion.

SUMMARY

The high- and low-temperature forms, namely, phases I and II, of Cu_8GeSe_6 have been investigated by powder diffraction methods. The superspace-group approach allows uniform treatment of both forms, and the phase transition of Cu_8GeSe_6 is explained in terms of the presence and absence of commensurate modulation waves. High-resolution powder data using a synchrotron X-ray source have made possible the analysis of individual thermal parameters for Cu ions in both phases. Though crystal structures of Cu_8GeSe_6 I and II have been already reported using the single-crystal X-ray method (9), the present investigation using modern theoretical and experimental techniques with powder data has revealed a fine capacity to explain the phase transition of Cu_8GeSe_6. This successful demonstration of the superspace-group approach opens up the way to a wider application of powder diffraction techniques for investigating complex structural phase transitions.

ACKNOWLEDGMENTS

We gratefully acknowledge the Swiss National Science Foundation for financial support and for access to the Swiss Norwegian beam line installed at the ESRF. We express appreciation to Dr. K. Kato, NIRIM, for valuable advice.

REFERENCES

1. C. Carcaly, N. Chèzeau, J. Rivet, and J. Flahaut, *Bull. Soc. Chim. Fr.* 1191 (1973).
2. H. Hahn, H. Schulze, and L. Sechster, *Naturwissenschaften* **52,** 451 (1965)

3. M. Khanafer, O. Gorochov, and J. Rivet, *Mater. Res. Bull.* **9,** 1543 (1974).
4. W. F. Kuhs, R. Nitsch, and K. Scheunemann, *Acta Crystallogr. B* **34,** 64 (1978).
5. W. F. Kuhs, R. Nitsch, and K. Scheunemann, *Mater. Res. Bull.* **14,** 241 (1979).
6. M. Levalois and G. Allais, *Acta Crystallogr.* **B37,** 1816 (1981).
7. M. Ishii, M. Onoda, and K. Shibata, *Solid State Ionics* **121,** 11 (1999).
8. M. Onoda, X.-a. Chen, K. Kato, A. Sato, and H. Wada, *Acta Crystallogr. B*, in press.
9. S. Jaulmes, M. Julien-Pouzol, P. Laruelle, and J. Rivet, *Acta Crystallogr.* **C41,** 1799 (1991).
10. A. Yamamoto, *Acta Crystallogr.* **A52,** 509 (1996).
11. K. Kato, *Acta Crystallogr.* **A50,** 351 (1994).
12. W. B. Pearson, "The Crystal Chemistry and Physics of Metals and Alloys," Wiley-Interscience, New York, 1972.
13. W. B. Pearson and C. B. Shoemaker, *Acta Crystallogr.* **B25,** 1178 (1969).
14. C. B. Shoemaker and D. P. Shoemaker, *Acta Crystallogr.* **B28,** 2957 (1972).
15. P. M. de Wolff, T. Janssen, and A. Janner, *Acta Crystallogr.* **A37,** 625 (1981).
16. A. Yamamoto, T. Janssen, A. Janner, and P. M. de Wolff, *Acta Crystallogr.* **A41,** 528 (1985).
17. "International Tables for Crystallography," Vol. C (A. J. C. Wilson, ed.), pp. 797–835. Kluwer Academic, Dordrecht, 1992.
18. S. van Smaalen, *Acta Crystallogr.* **A43,** 202 (1987).
19. P. M. de Wolff, *Acta Crystallogr.* **A30,** 777 (1974).